arXiv:1405.1327v1 [cond-mat.mtrl-sci] 6 May 2014

# Electrocaloric effect in $KH_2PO_4$

A.S.Vdovych[1], A.P.Moina[1], R.R.Levitskii[1], and I.R.Zachek[2]

[1]*Institute for Condensed Matter Physics, 79011, 1 Svientsitskii St, Lviv, Ukraine*

[2]*Lviv National Polytechnic University, 12 Bandery Street, 79013, Lviv, Ukraine*

**Abstract**

The proton ordering model for the $KH_2PO_4$ type ferroelectrics is modified by taking into account non-linear effects, namely, the dependence of the effective dipole moments on the proton ordering parameter. Within the four-particle cluster approximation we calculate the crystal polarization, longitudinal dielectric permittivity, specific heat, and explore the electrocaloric effect. Smearing of the ferroelectric phase transition by the longitudinal electric field is described. A good agreement with experiment is obtained.

Key words: electrocaloric effect, KDP, cluster approximation, polarization
PACS numbers: 77.84.Fa, 77.70.+a

## 1 Introduction

At the moment, the largest electrocaloric (EC) effect, which is the change of temperature of a dielectric at an adiabatic change of the applied electric field, is observed in perovskite ferroelectrics. Thus, in [1] in the $PbZr_{0.95}Ti_{0.05}O_3$ thin film with a thickness of 350 nm in a strong electric field (480 kV/cm) the obtained electrocaloric temperature change is $\Delta T = 12$ K. *Ab initio* molecular dynamics calculations [2] predict $\Delta T \approx 20$ K in $LiNbO_3$. In cheaper and more readily available hydrogen bonded ferroelectrics of the $KH_2PO_4$ (KDP) type the electrocaloric effect was studied for relatively low fields only. Thus, it has been obtained that $\Delta T \approx 0.04$ K at $E \approx 4$ kV/cm [3], $\Delta T \approx$ 1 K at $E \approx 12$ kV/cm [4], and $\Delta T \approx 0.25$ K at $T_c$ and $E \approx 1.2$ kV/cm [5]. The electrocaloric effect in KDP in high fields remains unexplored.

Theoretically the electrocaloric effect in KDP has been described in [6] within the Slater model [7] and in the paraelectric phase only. However, the Slater model is known to give incorrect results in the ferroelectric phase. Influence of electric field on the thermodynamic characteristics of the KDP type crystals, such as polarization, dielectric permittivity, piezoelectric coefficients, elastic constants has been described in [8,9,11] within the proton ordering model with the piezoelectric coupling to the shear strain $\varepsilon_6$ and proton tunneling [10] taken into account. However, these theories required, in particular,

invoking two different values of the effective dipole moments for the paraelectric and ferroelectric phase [8, 11]. This made a correct description of the system behavior in the fields high enough to smear out the first order phase transition impossible.

In the present paper we suggest a way to circumvent this difficulty. Assuming that the difference between the dipole moments is caused by non-zero values of the order parameter, we modify the proton ordering model accordingly. The crystal characteristics in zero field and in high fields are calculated. Smearing of the first order phase transition and the electrocaloric effect are described.

## 2 Thermodynamic characteristics

We consider the KDP type ferroelectrics in presence of the external shear stress $\sigma_6 = \sigma_{xy}$ and electric field $E_3$ applied along the crystallographic axis **c**, inducing the strain $\varepsilon_6$ and polarization $P_3$. The total model Hamiltonian reads [9]

$$\hat{H} = N\hat{H}_0 + \hat{H}_s, \tag{1}$$

where $N$ is the total number of primitive cells; The "seed" energy corresponds to the sublattice of heavy ions and does not depend explicitly on the deuteron subsystem configuration. It is expressed in terms of the strain $\varepsilon_6$ and electric field $E_3$ and includes the elastic, piezoelectric, and dielectric contributions

$$\hat{H}_0 = v\left(\frac{1}{2}c_{66}^{E0}\varepsilon_6^2 - e_{36}^0 E_3\varepsilon_6 - \frac{1}{2}\chi_{33}^{\varepsilon 0}E_3^2\right), \tag{2}$$

where $v$ is the primitive cell volume; $c_{44}^{E0}$, $e_{36}^0$, $\chi_{33}^{\varepsilon 0}$ are the "seed" elastic constant, piezoelectric coefficient, and dielectric susceptibility.

The pseudospin part of the Hamiltonian reads

$$\hat{H}_s = \frac{1}{2}\sum_{\substack{qf\\q'f'}} J_{ff'}(qq')\frac{\sigma_{qf}}{2}\frac{\sigma_{q'f'}}{2} + \hat{H}_{sh} + \sum_{qf} 2\psi_6\varepsilon_6\frac{\sigma_{qf}}{2} - \sum_{qf}\mu_f E_3\frac{\sigma_{qf}}{2} + \hat{H}_E. \tag{3}$$

Here the first term describes the effective long-range interactions between protons, including also indirect lattice-mediated interactions [12, 13], $\sigma_{qf}$ is the operator of the $z$-component of a pseudospin, corresponding to the proton on the $f$-th hydrogen bond ($f$=1,2,3,4) in the $q$-th cell. Its eigenvalues $\sigma_{qf} = \pm 1$ are assigned to two equilibrium positions of a proton on this bond

In (3) $\hat{H}_{sh}$ is the Hamiltonian of the short-range interactions between protons, which includes linear over the strain $\varepsilon_6$ terms [9, 11]

$$\begin{aligned}
\hat{H}_{sh} = \sum_q \Big\{ &\left(\frac{\delta_s}{8}\varepsilon_6 + \frac{\delta_1}{4}\varepsilon_6\right)(\sigma_{q1}+\sigma_{q2}+\sigma_{q3}+\sigma_{q4}) + \\
&+\left(\frac{\delta_s}{8}\varepsilon_6 - \frac{\delta_1}{4}\varepsilon_6\right)(\sigma_{q1}\sigma_{q2}\sigma_{q3}+\sigma_{q1}\sigma_{q2}\sigma_{q4}+\sigma_{q1}\sigma_{q3}\sigma_{q4}+\sigma_{q2}\sigma_{q3}\sigma_{q4}) + \\
&+\frac{1}{4}(V+\delta_a\varepsilon_6)(\sigma_{q1}\sigma_{q2}+\sigma_{q3}\sigma_{q4}) + \frac{1}{4}(V-\delta_a\varepsilon_6)(\sigma_{q2}\sigma_{q3}+\sigma_{q4}\sigma_{q1}) + \\
&+\frac{1}{4}U(\sigma_{q1}\sigma_{q3}+\sigma_{q2}\sigma_{q4}) + \frac{1}{16}\Phi\sigma_{q1}\sigma_{q2}\sigma_{q3}\sigma_{q4}\Big\}.
\end{aligned} \tag{4}$$

Here

$$V = -\frac{1}{2}w_1, \quad U = \frac{1}{2}w_1 - \varepsilon, \quad \Phi = 4\varepsilon - 8w + 2w_1,$$

where $\varepsilon$ $w$, $w_1$ are the energies of proton configurations.

The third term in (3) is a linear over the shear strain $\varepsilon_6$ field due to the piezoelectric coupling; $\psi_6$ is the deformational potential [9].

The fourth term in (3) effectively describes the system interaction with the external electric field $E_3$. Here $\mu_f$ is the effective dipole moment of the $f$-the hydrogen bond, and

$$\mu_1 = \mu_2 = \mu_3 = \mu_4 = \mu.$$

The fifth term in (3) is introduced in the present paper for the first time. It takes into account the dependence of the effective dipole moment on the order parameter (pseudospin mean value)

$$\hat{H}_E = -\frac{1}{N^2}\sum_{qf}\left(\sum_{q'f'}\frac{\sigma_{q'f'}}{2}\right)^2 \mu' E_3 \frac{\sigma_{qf}}{2}. \tag{5}$$

Considering the crystal structure of the KDP type ferroelectric, the four-particle cluster approximation is most suitable for the short-range interactions [13,14]. The long-range interactions and the term $\hat{H}_E$ are taken into account in the mean field approximation. Thus,

$$\hat{H}_E = -\frac{1}{N^2}\sum_{qf}\left(\sum_{q'f'}\frac{\sigma_{q'f'}}{2}\right)^2 \mu' E_3 \frac{\sigma_{qf}}{2} = -\frac{1}{N^2}\frac{\mu' E_3}{8}\sum_{qf}\sum_{q'f'}\sum_{q''f''}\sigma_{qf}\sigma_{q'f'}\sigma_{q''f''} \approx$$
$$-\frac{1}{N^2}\frac{\mu' E_3}{8}\sum_{qf}\sum_{q'f'}\sum_{q''f''}((\sigma_{qf} + \sigma_{q'f'} + \sigma_{q''f''})\eta^2 - 2\eta^3) =$$
$$-N\frac{\mu' E_3}{8}\sum_{f=1}^{4}\sum_{f'=1}^{4}\sum_{f''=1}^{4}((\sigma_f + \sigma_{f'} + \sigma_{f''})\eta^2 - 2\eta^3) =$$
$$-12N\mu' E_3\sum_{f=1}^{4}\frac{\sigma_{qf}}{2}\eta^2 + 16N\mu' E_3\eta^3. \tag{6}$$

The calculated thermodynamic potential per one primitive cell reads

$$G = H^{(0)} + 2\nu_c\eta^2 + 16\mu' E_3\eta^3 + \frac{1}{2\beta}\sum_{f=1}^{4}\ln Z_{1f} - \frac{1}{\beta}\ln Z_4 - v\sigma_6\varepsilon_6, \tag{7}$$

where $4\nu_c = J_{11}(0) + 2J_{12}(0) + J_{13}(0)$ is the eigenvalue of the long-range interactions matrix Fourier transform $J_{ff'} = \sum\limits_{\mathbf{R}_q - \mathbf{R}_{q'}} J_{ff'}(qq')$;

$$\eta = \langle\sigma_{q1}\rangle = \langle\sigma_{q2}\rangle = \langle\sigma_{q3}\rangle = \langle\sigma_{q4}\rangle$$

is the proton ordering parameter; $Z_{1f} = Spe^{-\beta\hat{H}_{qf}^{(1)}}$, $Z_4 = Spe^{-\beta\hat{H}_q^{(4)}}$ are the single-particle and four-particle partition functions; $\beta = \frac{1}{k_B T}$. The single-particle $\hat{H}_{qf}^{(1)}$ and four-particle $\hat{H}_{q6}^{(4)}$ proton Hamitonians are

$$\hat{H}_{qf}^{(1)} = -\frac{\bar{z}_f}{\beta}\frac{\sigma_{qf}}{2}, \tag{8}$$

$$\hat{H}_q^{(4)} = -\sum_{f=1}^{4}\frac{z}{\beta}\frac{\sigma_{qf}}{2} + \frac{\varepsilon_6}{4}(-\delta_s + 2\delta_1)\sum_{f=1}^{4}\frac{\sigma_{qf}}{2} - \tag{9}$$
$$-\varepsilon_6(\delta_s+2\delta_1)\Big(\frac{\sigma_{q1}}{2}\frac{\sigma_{q2}}{2}\frac{\sigma_{q3}}{2}+\frac{\sigma_{q1}}{2}\frac{\sigma_{q2}}{2}\frac{\sigma_{q4}}{2}+\frac{\sigma_{q1}}{2}\frac{\sigma_{q3}}{2}\frac{\sigma_{q4}}{2}+\frac{\sigma_{q2}}{2}\frac{\sigma_{q3}}{2}\frac{\sigma_{q4}}{2}\Big) +$$
$$+(V+\delta_a\varepsilon_6)\left(\frac{\sigma_{q1}}{2}\frac{\sigma_{q2}}{2}+\frac{\sigma_{q3}}{2}\frac{\sigma_{q4}}{2}\right)+(V-\delta_a\varepsilon_6)\left(\frac{\sigma_{q2}}{2}\frac{\sigma_{q3}}{2}+\frac{\sigma_{q4}}{2}\frac{\sigma_{q1}}{2}\right)+$$
$$+U\left(\frac{\sigma_{q1}}{2}\frac{\sigma_{q3}}{2}+\frac{\sigma_{q2}}{2}\frac{\sigma_{q4}}{2}\right)+\Phi\frac{\sigma_{q1}}{2}\frac{\sigma_{q2}}{2}\frac{\sigma_{q3}}{2}\frac{\sigma_{q4}}{2},$$

where

$$z = \beta[-\Delta^c + 2\nu_c\eta - 2\psi_6\varepsilon_6 + \mu E_3 + 12\mu'\eta^2 E_3],$$
$$\bar{z}_f = \beta[-2\Delta^c + 2\nu_c\eta - 2\psi_6\varepsilon_6 + \mu E_3 + 12\mu'\eta^2 E_3].$$

The effective field $\Delta^c$ exerted by the neighboring hydrogen bonds from outside the cluster can be determined from the self-consistency condition: the pseudospin mean value $\langle\sigma_{qf}\rangle$ calculated with the four-particle and with the one-particle Hamiltonians must coincide

$$\langle\sigma_{qf}\rangle = \frac{\mathrm{Sp}\left\{\sigma_{qf}e^{-\beta\hat{H}_q^{(4)}}\right\}}{\mathrm{Sp}\,e^{-\beta\hat{H}_q^{(4)}}} = \frac{\mathrm{Sp}\left\{\sigma_{qf}e^{-\beta\hat{H}_{qf}^{(1)}}\right\}}{\mathrm{Sp}\,e^{-\beta\hat{H}_{qf}^{(1)}}}. \tag{10}$$

Finally, the order parameter is

$$\eta = \frac{m}{D}, \tag{11}$$

where

$$m = \sinh(2z + \beta\delta_s\varepsilon_6) + 2b\sinh(z - \beta\delta_1\varepsilon_6),$$
$$D = \cosh(2z + \beta\delta_s\varepsilon_6) + 4b\cosh(z - \beta\delta_1\varepsilon_6) + 2a\cosh\beta\delta_a\varepsilon_6 + d,$$
$$z = \frac{1}{2}\ln\frac{1+\eta}{1-\eta} + \beta\nu_c\eta - \beta\psi_6\varepsilon_6 + \frac{\beta\mu}{2}E_3 + 6\beta\mu'\eta^2E_3,$$
$$a = e^{-\beta\varepsilon}, \quad b = e^{-\beta w}, \quad d = e^{-\beta w_1}.$$

The thermodynamic potential (7) is then obtained in the following form

$$G = \frac{v}{2}c_{66}^{E0}\varepsilon_6^2 - ve_{36}^0\varepsilon_6E_3 - \frac{v}{2}\chi_{33}^{\varepsilon 0}E_3^2 + 2\nu_c\eta^2 + 16\mu'E_3\eta^3 + \tag{12}$$
$$+\frac{2}{\beta}\ln 2 - \frac{2}{\beta}\ln[1-\eta^2] - \frac{2}{\beta}\ln D - v\sigma_6\varepsilon_6.$$

From the condition of the thermodynamic potential minimum

$$\left(\frac{\partial G}{\partial\varepsilon_6}\right)_{T,E_3,\sigma_6} = 0$$

we obtain an equation for the strain $\varepsilon_6$

$$\sigma_6 = c_{66}^{E0}\varepsilon_6 - e_{36}^0E_3 + \frac{4\psi_6}{v}\eta + \frac{2r}{vD}. \tag{13}$$

In the same way we derive the expressions for polarization $P_3$ and molar entropy of the proton subsystem

$$P_3 = -\frac{1}{v}\left(\frac{\partial G}{\partial E_3}\right)_{T,\sigma_6} = e_{36}^0\varepsilon_6 + \chi_{33}^{\varepsilon 0}E_3 + 2\frac{\mu}{v}\eta + 8\frac{\mu'}{v}\eta^3, \tag{14}$$

$$S = -\frac{N_A}{2}\left(\frac{\partial G}{\partial T}\right)_{E_3,\sigma_6} = R\left\{-\ln 2 + \ln[1-\eta^2] + \ln D + 2Tz_T\eta + \frac{M}{D}\right\}. \tag{15}$$

Here $N_A$ is the Avogadro number; $R$ is the gas constant. The following notations are used

$$\begin{aligned}
&r = -\delta_s M_s - \delta_a M_a + \delta_1 M_1,\\
&z_T = -\frac{1}{k_B T^2}(\nu_c\eta - \psi_6\varepsilon_6 + 6\mu'\eta^2 E_3),\\
&M = 4b\beta w\cosh(z-\beta\delta_1\varepsilon_6) + \beta w_1 d + 2a\beta\varepsilon\cosh\beta\delta_a\varepsilon_6 + \beta\varepsilon_6 r,\\
&M_a = 2a\sinh\beta\delta_a\varepsilon_6,\, M_s = \sinh(2z+\beta\delta_s\varepsilon_6),\, M_1 = 4b\sinh(z-\beta\delta_1\varepsilon_6).
\end{aligned}$$

From Eqs. (13), (14) we find the isothermal dielectric susceptibility of a clamped crystal ($\varepsilon_6 = \text{const}$):

$$\chi_{33}^{T\varepsilon} = \left(\frac{\partial P_3}{\partial E_3}\right)_{T,\varepsilon_6} = \chi_{33}^0 + \frac{(\mu+12\mu'\eta^2)^2}{v}\frac{2\beta\varkappa}{D-2\varkappa z_\eta}, \tag{16}$$

where

$$\begin{aligned}
&\varkappa = \cosh(2z+\beta\delta_s\varepsilon_6) + b\cosh(z-\beta\delta_1\varepsilon_6) - \eta m,\\
&z_\eta = \frac{1}{1-\eta^2} + \beta\nu_c + 12\beta\mu'\eta E_3;
\end{aligned}$$

the isothermal piezoelectric coefficient $e_{36}^T$

$$e_{36}^T = -\left(\frac{\partial\sigma_6}{\partial E_3}\right)_{T,\varepsilon_6} = \left(\frac{\partial P_3}{\partial\varepsilon_6}\right)_{T,E_3} = e_{36}^0 + \frac{2(\mu+12\mu'\eta^2)}{v}\frac{\beta\theta_6}{D-2z_\eta\varkappa}. \tag{17}$$

where

$$\theta_6 = -2\varkappa\psi_6 + f_6, \qquad f_6 = \delta_s\cosh(2z+\beta\delta_s\varepsilon_6) - 2b\delta_1\cosh(z-\beta\delta_1\varepsilon_6) + \eta r;$$

the isothermal elastic constant at constant field

$$\begin{aligned}
c_{66}^{TE} = c_{66}^{E0} + \frac{8\psi_6}{v}\frac{\beta(-\psi_6\varkappa + f_6)}{D-2z_\eta\varkappa} - \frac{4\beta z_\eta f_6^2}{vD(D-2z_\eta\varkappa)} - \\
-\frac{2\beta}{vD}[\delta_s^2\cosh(2z+\beta\delta_s\varepsilon_6) + 2a\delta_a^2\cosh\beta\delta_a\varepsilon_6 + 4b\delta_1^2\cosh(z-\beta\delta_1\varepsilon_6)] + \frac{2\beta r^2}{vD^2}.
\end{aligned} \tag{18}$$

Other isothermal dielectric and piezoelectric characteristics can be expressed via those found above, using the known thermodynamic relations. Thus, the isothermal dielectric susceptibility of a free crystal ($\sigma_6$=const)

$$\chi_{33}^{T\sigma} = \left(\frac{\partial P_3}{\partial E_3}\right)_{T,\sigma_6} = \chi_{33}^{T\varepsilon} + \frac{(e_{36}^T)^2}{c_{66}^{TE}} = \chi_{33}^{T\varepsilon} + e_{36}^T d_{36}^T, \tag{19}$$

isothermal piezoelectric coefficient

$$d_{36}^T = \left(\frac{\partial \varepsilon_6}{\partial E_3}\right)_{T,\sigma_6} = \left(\frac{\partial P_3}{\partial \sigma_6}\right)_{T,E_3} = \frac{e_{36}^T}{c_{66}^{TE}}, \tag{20}$$

The molar specific heat of the proton subsystem is

$$\Delta C^\sigma = T\left(\frac{\partial S}{\partial T}\right)_\sigma = T(S_T + S_\eta \eta_T + S_\varepsilon \varepsilon_T), \tag{21}$$

Here we used the following notations

$$\begin{aligned}
S_T &= \left(\frac{\partial S}{\partial T}\right)_{P_3,\varepsilon_6} = \frac{R}{DT}\left\{2Tz_T(q_6 - \eta M) + N_6 - \frac{M^2}{D}\right\}, \\
S_\eta &= \left(\frac{\partial S}{\partial \eta}\right)_{\varepsilon_6,T} = \frac{2R}{D}\{DTz_T + [q_6 - \eta M]z_\eta\} \\
S_\varepsilon &= \left(\frac{\partial S}{\partial \varepsilon_6}\right)_{\eta,T} = \frac{R}{k_B T D}\left\{-2[q_6 - \eta M]\psi_6 - \lambda + \frac{M}{D}r\right\},
\end{aligned} \tag{22}$$

$$\begin{aligned}
&N_6 = 2a(\beta\varepsilon)^2 \cosh\beta\delta_a\varepsilon_6 + 4b(\beta w)^2\cosh(z - \beta\delta_1\varepsilon_6) + (\beta w_1)^2 d + \\
&+2\beta^2\varepsilon_6(-\varepsilon\delta_a M_a + w\delta_1 M_1) + \\
&+\varepsilon_6^2[2a(\beta\delta_a)^2\cosh\beta\delta_a\varepsilon_6 + (\beta\delta_s)^2\cosh(2z + \beta\delta_s\varepsilon_6) + 4b(\beta\delta_1)^2\cosh(z - \beta\delta_1\varepsilon_6)], \\
&q_6 = 2b\beta w\sinh(z - \beta\delta_1\varepsilon_6) + \beta\varepsilon_6[-\delta_s\cosh(2z + \beta\delta_s\varepsilon_6) + 2b\delta_1\cosh(z - \beta\delta_1\varepsilon_6)], \\
&\lambda = -\beta\varepsilon\delta_a M_a + \beta w\delta_1 M_1 + \\
&+\varepsilon_6\beta[\delta_s^2\cosh(2z + \beta\delta_s\varepsilon_6) + 2a\delta_a^2\cosh\beta\delta_a\varepsilon_6 + 4b\delta_1^2\cosh(z - \beta\delta_1\varepsilon_6)], \\
&\eta_T = p_6^\varepsilon + \frac{v}{2(\mu + 12\mu'\eta^2)}[e_{36}^T - e_{36}^0]\varepsilon_T, \\
&\varepsilon_T = \left(\frac{2}{vDT}(2Tz_T f_6 - \lambda + \frac{Mr}{D}) - \frac{4p_6^\varepsilon}{v}(\psi_6 - \frac{z_\eta f_6}{D})\right)/c_{66}^{TE}, \\
&p_6^\varepsilon = \frac{1}{T}\frac{2\varkappa T z_T + [q_6 - \eta M]}{D - 2\varkappa z_\eta}.
\end{aligned} \tag{23}$$

The total specific heat is the sum of the proton and lattice contributions

$$C = \Delta C^\sigma + C_{lattice} \tag{24}$$

The lattice heat capacity near $T_c$ is approximated by a linear dependence

$$C_{lattice} = C_0 + C_1(T - T_c) \tag{25}$$

Then the lattice entropy near $T_c$ is

$$S_{lattice} = \int \frac{C_{lattice}}{T}dT = (C_0 - C_1 T_c)\ln(T) + C_1 T + const \tag{26}$$

The total entropy is a function of temperature and electric field

$$S_{total}(T, E) = S + S_{lattice} \tag{27}$$

Solving Eq.(27) with respect to temperature at $S_{total}(T,E) = const$ and two different fields, we can find the electrocaloric temperature change

$$\Delta T = T(S_{total}, E_2) - T(S_{total}, E_1). \tag{28}$$

Alternatively, the electrocaloric temperature change can be calculated using the know formula

$$\Delta T = \int_0^E \frac{TV}{C} \left(\frac{\partial P_3}{\partial T}\right)_E dE; \tag{29}$$

where the pyroelectric coefficient is

$$\left(\frac{\partial P_3}{\partial T}\right)_E = (e_{36}^0 \varepsilon_T + \frac{2(\mu + 12\mu'\eta^2)}{v}\eta_T); \tag{30}$$

$V = vN_A/2$ is the molar volume.

# 3 Numerical calculations

To perform the numerical calculations we need to set the values of the following theory parameters

- The Slater energies $\varepsilon$, $w$, $w_1$ ;
- the parameter of the long-range interactions $\nu_c$;
- the effective dipole moment $\mu$;
- the correction to the effective dipole moment due to proton ordering $\mu'$;
- the deformation potentials $\psi_6$, $\delta_s$, $\delta_a$, $\delta_1$;
- the "seed" dielectric susceptibility $\chi_{33}^{\varepsilon 0}$;
- the "seed" elastic constant $c_{66}^{E0}$;
- the "seed" piezoelectric coefficient $e_{36}^0$.

They are chosen, obviously, by fitting the theoretical thermodynamic characteristics to the experimental data, as described in [11].

The energy $w_1$ of two proton configurations with four or zero protons near the given oxygen tetrahedron should be much higher than $\varepsilon$ and $w$. Therefore we take $w_1 = \infty$ $(d = 0)$.

The optimum sets of the model parameters are given in Table 1. $T_c^0$ is phase transition temperature at zero field.

The primitive cell volume is taken to be $v = 0.195 \cdot 10^{-21}$ cm$^3$ for all compositions. The values of the lattice specific heat parameters of are $C_0 = 60$ J/(mol K), $C_1 = 0.32$ J/(mol K$^2$) for $x = 0$ and $C_0 = 93$ J/(mol K), $C_1 = 0.32$ J/(mol K$^2$) for $x = 0.86$ and 0.89.

When the dependence of the effective dipole moment on the order parameter is taken into account, the agreement between the theory and experiment for most of the calculated

Table 1: The optimum sets of the model parameters for $K(H_{1-x}D_x)_2PO_4$.

| $x$ | $T_c^0$ (K) | $\frac{\varepsilon}{k_B}$ (K) | $\frac{w}{k_B}$ (K) | $\frac{\nu_c}{k_B}$ (K) | $\mu$ ($10^{-30}$ C·m) | $\mu'$ ($10^{-30}$ C·m) | $\chi_{33}^0$ |
|---|---|---|---|---|---|---|---|
| 0.00 | 122.22 | 56.00 | 430.0 | 17.55 | 5.6 | -0.217 | 0.75 |
| 0.84 | 208.00 | 83.68 | 713.5 | 38.73 | 6.8 | -0.217 | 0.41 |
| 0.88 | 211.00 | 85.00 | 727.0 | 39.17 | 6.8 | -0.217 | 0.39 |
| 0.89 | 211.73 | 85.33 | 730.4 | 39.26 | 6.8 | -0.217 | 0.39 |

| $x$ | $\frac{\psi_6}{k_B}$ (K) | $\frac{\delta_s}{k_B}$ (K) | $\frac{\delta_a}{k_B}$ (K) | $\frac{\delta_1}{k_B}$ (K) | $c_{66}^{E0}$ ($10^9$ N/m$^2$) | $e_{36}^0$ (C/m$^2$) |
|---|---|---|---|---|---|---|
| 0.00 | -150.00 | 82.00 | -500.00 | -400.00 | 7.00 | 0.0033 |
| 0.84 | -140.45 | 51.45 | -977.27 | -400.00 | 6.43 | 0.0033 |
| 0.88 | -140.00 | 50.00 | -1000.00 | -400.00 | 6.40 | 0.0033 |
| 0.89 | -139.89 | 48.64 | -1005.68 | -400.00 | 6.39 | 0.0033 |

thermodynamic characteristics of $K(H_{1-x}D_x)_2PO_4$ crystals in absence of the external electric field is neither improved nor worsened. Thus, the calculated temperature dependences of the inverse static dielectric permittivities of free $(\varepsilon_{33}^{\sigma})^{-1}$ and clamped $(\varepsilon_{33}^{\varepsilon})^{-1}$ crystals (figs. 1, 2), piezoelectric coefficient $d_{36}$ (fig. 3), and molar specific heat (fig. 4) are close to the previous theoretical curves [11].

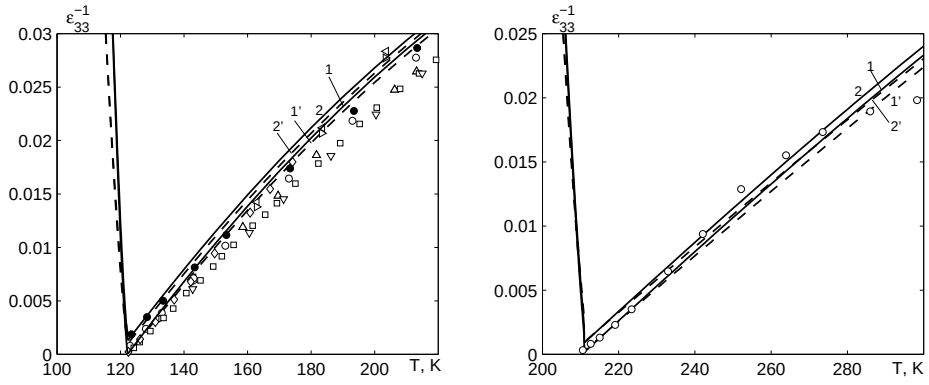


Figure 1: The temperature dependence of the inverse static dielectric permittivities of free $(\varepsilon_{33}^{\sigma})^{-1}$ and clamped $(\varepsilon_{33}^{\varepsilon})^{-1}$ $K(H_{1-x}D_x)_2PO_4$ crystals at $x = 0.0$. Symbols are experimental data taken from ∘, • – [19], □ – [20], ◊ – [21], ▷ – [22], ◁ – [15], ▽ – [23], △ [24]. Solid lines: the present theory; dashed lines: the theoretical results of [11] for $(\varepsilon_{33}^{\sigma})^{-1}$ (1') and $(\varepsilon_{33}^{\varepsilon})^{-1}$ (2').

Figure 2: The same for $x = 0.88$. Symbols are experimental data taken from ∘ – [25].

However, the present model allows us to describe more consistently the smearing of the first order phase in high electric fields. In figs. 5, 6, and 7 we plotted the temperature variation of the polarization of $K(H_{1-x}D_x)_2PO_4$ in different fields.

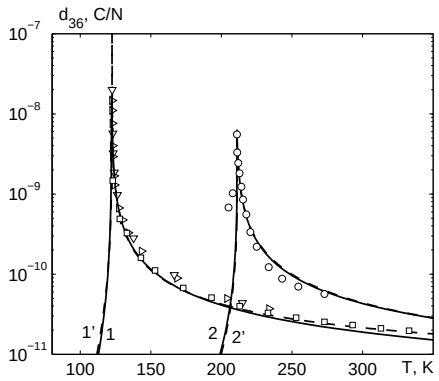


Figure 3: The temperature dependence of the piezoelectric coefficient $d_{36}$ of $K(H_{1-x}D_x)_2PO_4$ at $x = 0.0$ – 1, 1', □ [19], ▽ [26], ▷, [27]; at $x = 0.88$ – 2, 2', ○ [25]. Dashed lines: the theoretical results of [11].

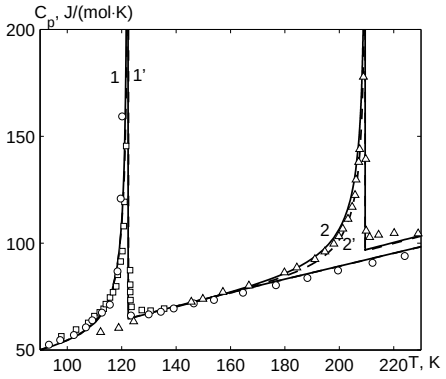


Figure 4: The temperature dependence of the molar specific heat of $K(H_{1-x}D_x)_2PO_4$ at $x = 0.0$ – ○ [17], □ [18]; at $x = 0.86$ – △ [18]. Dashed lines: the theoretical results of [11].

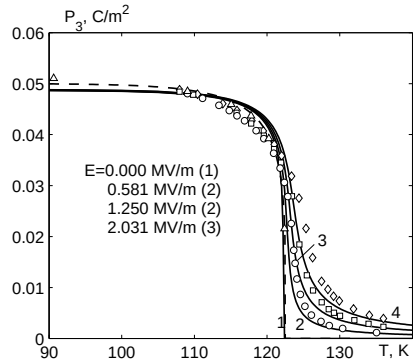


Figure 5: The temperature dependence of polarization of $K(H_{1-x}D_x)_2PO_4$ at $x = 0$ and at different $E_3$(MV/m): 0.0 – 1, △ [3]; 0.581 – 2, ○ [15]; 1.250 – 3, □ [15]; 2.031 – 4, ◇ [15]. Symbols are experimental points; solid lines: the present theory; dashed lines: the theoretical results of [11].

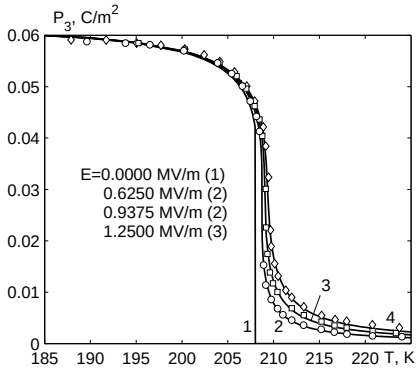


Figure 6: The temperature dependence of polarization of $K(H_{1-x}D_x)_2PO_4$ at $x = 0.84$ and at different $E_3$(MV/m): 0.0 – 1; 0.625 – 2, ∘; 0.9375 – 3, □; 1.25 – 4, ◊. Symbols are experimental points; lines: the present theory.

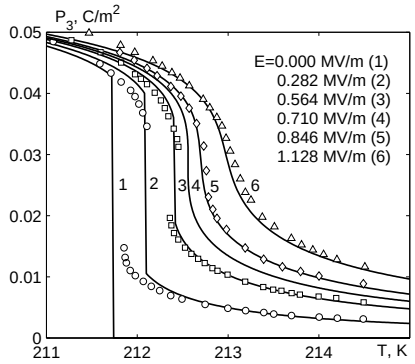


Figure 7: The temperature dependence of polarization of $K(H_{1-x}D_x)_2PO_4$ at $x = 0.89$ and at different $E_3$ (MV/m): 0.0 – 1; 0.282 – 2, ∘; 0.564 – 3, □; 0.71 – 4; 0.846 – 5, ◊; 1.128 – 6, △. Symbols are experimental points taken from [16]; lines: the present theory.

The agreement with experiment is better at $x = 0.84$ and 0.89 than at $x = 0$. We believe this is due to proton tunnelling, essential in non-deuterated samples, which is not included in our model. The field $E_3$, which in these crystals is the field conjugate to the order parameter, induces non-zero polarization $P_3$ above the transition point. Polarization has a jump at $T_c$, indicating the first order phase transition. With increasing field, the polarization jump decreases, whereas the transition temperature $T_c$ increases almost linearly. The corresponding $\partial T_c/\partial E_3$ slopes are 0.192 and 0.115 K cm/kV for $x = 0$ and $x = 0.89$, respectively (c.f. 0.22 and 0.13 K cm/kV from our earlier calculations [8] and experimental 0.125 K cm/kV of [29] for $x = 0.89$). At some critical field $E^*$ the jump vanishes, and the transition smears out. The calculated coordinates of the critical point are $E^* = 125$ V/cm, $T_c^*$=122.244 K for $x = 0$ and 7.1 kV/cm, 212.55 K for $x = 0.89$, which agrees well with the experiment [28, 29]. It should be noted that in our previous calculations [11] it was impossible to obtain a correct description of the polarization behavior in the fields above the critical one, because of the necessity to use two different values of the effective dipole moment $\mu$ in calculations.

Smearing of the phase transition is observed also in the temperature dependences of the dielectric permittivity $\varepsilon_{33}$ (fig. 8), piezoelectric coefficient $d_{36}$ (fig. 9), and elastic constant $c_{66}^E$ (fig. 10).

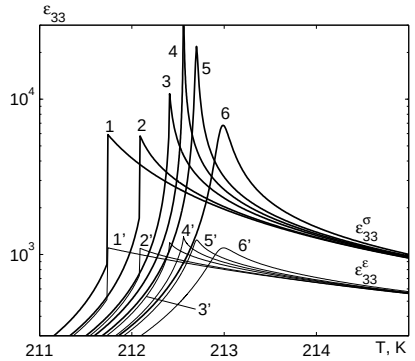


Figure 8: The temperature dependence of the inverse static dielectric permittivities of free $(\varepsilon_{33}^{\sigma})^{-1}$ (bold lines) and clamped $(\varepsilon_{33}^{\varepsilon})^{-1}$ (thin lines) $K(H_{1-x}D_x)_2PO_4$ crystals for $x = 0.89$ at different electric fields $E_3$ (MV/m): 0.0 – 1, 1'; 0.282 – 2, 2'; 0.564 – 3, 3'; 0.71 – 4, 4'; 0.846 – 5, 5'; 1.128 – 6, 6'.

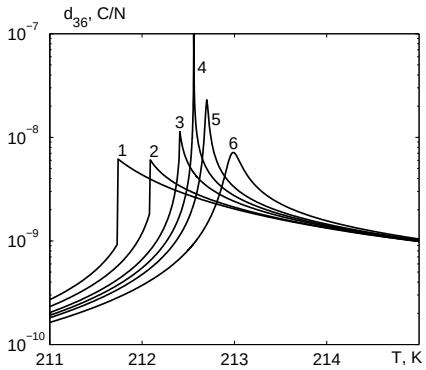


Figure 9: The temperature dependence of the piezoelectric coefficient $d_{36}$ of $K(H_{1-x}D_x)_2PO_4$ for $x = 0.89$ at different electric fields $E_3$ (MV/m): 0.0 – 1, 1'; 0.282 – 2, 2'; 0.564 – 3, 3'; 0.71 – 4, 4'; 0.846 – 5, 5'; 1.128 – 6, 6'.

The calculated changes of temperature $\Delta T$ of the KDP crystals with the adiabatically applied electric field is showin in figs. 11, 12, and 13. As one can see, at small fields (fig. 11) the calculated electrocaloric temperature change is a linear function of the field in the ferroelectric (curves 1, 1′) and a quadratic function in the paraelectric phase (curves 2, 2′). The experimental behavior in the ferroelectric phase is not linear at $E < 3$ kV/cm because of the domains. The experimental data of [5] (fig. 12) were obtained at $T = 121$ K, which was very close to the transition temperature of the sample used in the measurements. The domains, which polarization is oriented along the field, are heated, whereas the domains, polarized in the opposite direction are cooled. The disagreement between the theory and experiment for an undeuterated crystal in the ferroelectric phase can be also caused by tunneling, which is not taken into account in the present model. In very

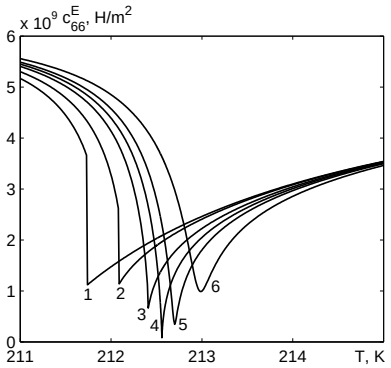


Figure 10: The temperature dependence of the elastic constant $c_{66}^E$ of $K(H_{1-x}D_x)_2PO_4$ for $x = 0.89$ at different electric fields $E_3$ (MV/m): 0.0 – 1, 1'; 0.282 – 2, 2'; 0.564 – 3, 3'; 0.71 – 4, 4'; 0.846 – 5, 5'; 1.128 – 6, 6'.

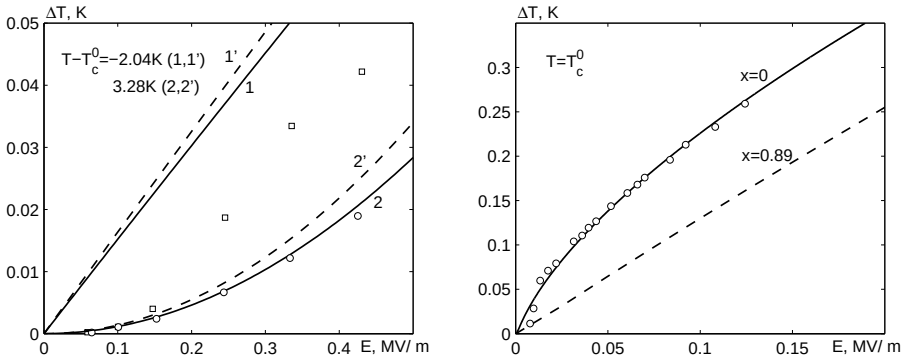


Figure 11: The field dependences of the electrocaloric temperature change of $K(H_{1-x}D_x)_2PO_4$ for $x = 0.0$ (solid lines) in the ferroelectric phase at $T - T_c^0 = -2.04$ K – 1, □ [3] and in the paraelectric phase at $T - T_c^0 = 3.28$ K – 2, ∘ [3]; for $x = 0.89$ (dashed lines) $T - T_c^0 = -2.04$ K – 1' and $T - T_c^0$=3.28K – 2'.

Figure 12: The field dependence of the electrocaloric temperature change of $K(H_{1-x}D_x)_2PO_4$ at $T = T_c^0$ for $x = 0.0$ (solid line, ∘ [5]) and $x = 0.89$ (dashed line).

high fields (fig. 13) the calculated electrocaloric temperature change in the paraelectric phase are larger than in the ferroelectric phase. The obtained curves deviate from linear and quadratic behavior and reach saturation at $E \gg 50$ MV/m. To create fields that high in macroscopic single crystals is obviously practically impossible, because of the dielectric breakdown. However, experimental data for $\Delta T$ are not available even for moderate fields above 0.5 MV/m.

As one can see from the temperature dependence of $\Delta T$ (fig. 14), the calculated electrocaloric temperature change is the largest in the paraelectric phase close to $T_c$ and can exceed 6 K. The electrocaloric effect in $K(H_{1-x}D_x)_2PO_4$ at $x = 0.89$ is larger than at $x = 0.0$, because with increasing deuteration the first order character of the phase transitions becomes more pronounced.

We can also find $\Delta T$ using Eq. (28), that is, as illustrated in fig. 15. The values of

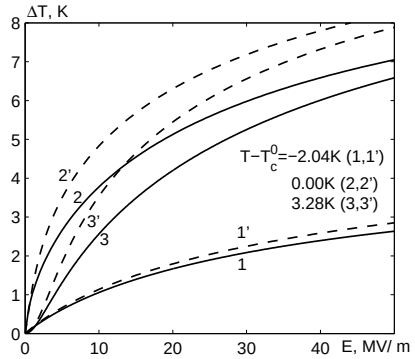


Figure 13: The field dependence of the electrocaloric temperature change of $K(H_{1-x}D_x)_2PO_4$ for $x = 0.0$ (solid lines) and $x = 0.89$ (dashed lines) at $T - T_c^0 = -2.04$ K – 1, 1′; $T = T_c^0$ – 2, 2′; $T - T_c^0 = 3.2$ K – 3, 3′ for very high fields.

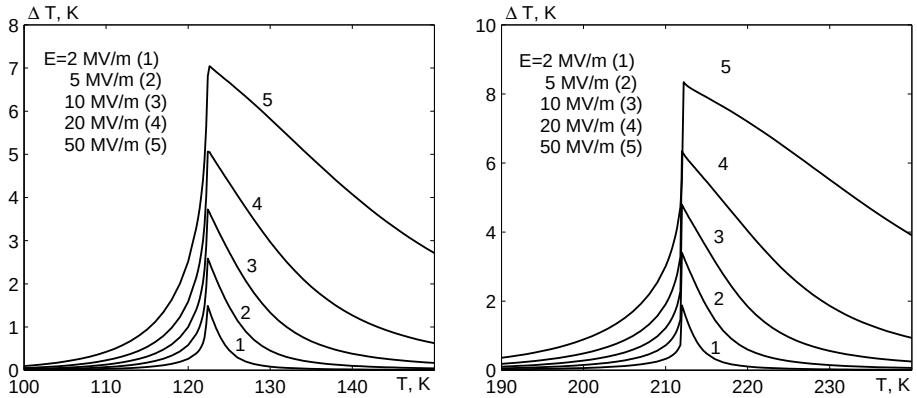


Figure 14: The temperature dependence of the electrocaloric temperature change of $K(H_{1-x}D_x)_2PO_4$ for $x = 0.0$ (left) and $x = 0.89$ (right) in different fields.

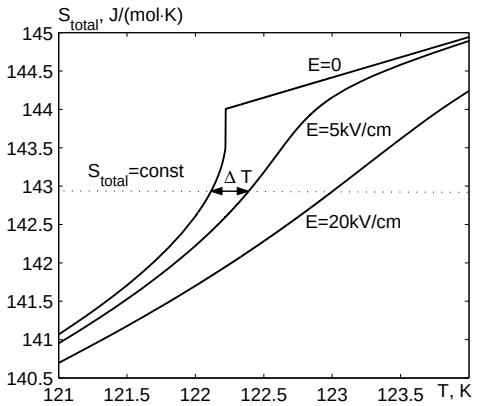


Figure 15: The temperature dependence of molar entropy of KDP at different fields.

$\Delta T$ calculated using Eqs. (29) and (28) coincide.

# 4 Conclusions

Taking into account the dependence of the effective dipole moment on the order parameter allows us to correctly describe smearing of the ferroelectric phase transition in high electric field as well as the electrocaloric effect in KDP crystals. The theory predicts the values of the electrocaloric temperature change above 5 K in very high fields. This fact could make the KDP crystals a promising material for electrocaloric refridgerators. Additional experimental measurements of $\Delta T$ in fields above 0.5 MV/m are necessary.

# References


[1] A.S. Mischenko, Q. Zhang, J.F. Scott, R.W. Whatmore, N.D. Mathur. Giant Electrocaloric Effect in Thin-Film $PbZr_{0.95}Ti_{0.05}O_3$ // Science. – 2006. – Vol.311. – P. 1270-1271.

[2] M.C. Rose, R.E. Cohen. Giant Electrocaloric Effect Around $T_c$ // Phys. Rev. Lett. – 2012. – Vol. 109. – P.187604 (5p.).

[3] G.G. Wiseman, IEEE Transactions on Electron Devices, **16**, 588 (1969).

[4] Baumgartner, H. // Helv. phys. acta. – 1950. – Vol.23. – P. 651-696.

[5] Shimshoni M. Harnik E. Ultrasonic measurement of the electrocaloric effect in $KH_2PO_4$ // J. Phys. Chem.Solids. – 1969. – Vol.31. – P.1416-1417.

[6] L.J. Dunne, M.Valant, G.Manos, A.-K. Axelsson, N. Alford. Microscopic theory of the electrocaloric effect in the paraelectric phase of potassium dihydrogen phosphate // Appl. Phys. Lett. – 2008. – Vol.93. – P.122906 (3p.)

[7] Slater J.C. Theory of the transition in $KH_2PO_4$ // J. Chem. Phys. - 1941. - Vol. 9, No 1. - P. 16-33.

[8] Stasyuk I.V., Levitskii R.R., Moina A.P., Lisnii B.M. Longitudinal field influence on phase transition and physical properties of the $KH_2PO_4$ family ferroelectrics. // Ferroelectrics, 2001, v. 254, p. 213–227.

[9] Stasyuk I.V., Levitskii R.R., Zachek I.R., Moina A.P. The $KD_2PO_4$ ferroelectrics in external fields conjugate to the order parameter: Shear stress $\sigma_6$. // Phys. Rev. B, 2000, v. 62, No 10, p. 6198–6207.

[10] B.M. Lisnii, R.R. Levitskii, O.R. Baran. Influence of electric field $E_3$ and mechanical shear stress $\sigma_6$ on $KD_2PO_4$ crystal ferroelectric phase transition // Phase Transitions. – 2007. – Vol. 80. P.25-30.

[11] Levitsky R.R., Zachek I.R., Vdovych A.S., Moina A.P. Longitudinal dielectric, piezoelectric, elastic, and thermal characteristics of the $KH_2PO_4$ type ferroelectrics // J. Phys. Studies. - 2010. - Vol. 14, No 1. - P. 1701(17p.)

[12] Stasyuk I.V., Levitskii R.R. The role proton-phonon Interaction in the phase transition of ferroelectrics with hydrogen bonds // Phys. Stat. Sol.b. – 1970. – Vol. 39, No 1. – P. K35-K38.

[13] Levitskii R.R., Korinevski N.A., Stasyuk I.V. // Ukr. Journ. Phys. – 1974. – vol. 19, – p. 1289-1297.

[14] Blinc R., Svetina S. Cluster approximation for order-disorder- type hydrogen-bounded ferroelectrics II. Application to $KH_2PO_4$ // Phys. Rev. – 1966. – Vol. 147, No 2. – P. 430-438.

[15] Chabin M., Gilletta F. Polarization and dielectric constant of KDP-type crystals // Ferroelectrics. - 1977. - Vol. 15. - P. 149-154.

[16] E.V. Sidnenko and V.V. Gladkii, Kristallografiya **17**, 978 (1972) [Sov. Phys. Crystallogr. **17**, 861 (1973)]

[17] Stephenson C.C., Hooly G.J. The Heat Capacity of Potassium Dihydrogen Phosphate from 15 to 300K. The Anomaly at the Curie Temperature // J. Am. Chem. Soc. – 1944. – Vol. 66, No.8. – P. 1397-1401.

[18] Strukov B.A., Baddur A., Koptsik V.A., Velichko I.A. // Solid State Phys. – 1972. – vol.14, No 4. – p. 1034-1039.

[19] W. P. Mason, Piezoelectric Constants and Their Application to Ultrasonics (Van Nostrand, New York, 1950).

[20] Deguchi K., Nakamura E. Deviation from the Curie-Weiss law in $KH_2PO_4$ // J.Phys.Soc.Japan. -1980. - Vol. 49, No 5. -P. 1887-1891.

[21] Samara G.A. The effects of deuteration on the static ferroelectric properties of $KH_2PO_4$ (KDP) // Ferroelectrics. - 1973. - Vol. 5. - P. 25-37.

[22] Vasilevskaya A.S., Sonin A.S. // Solid State Phys. – 1971. – vol.13, – p. 1550-1556.

[23] Mayer R.J., Bjorkstam J.L. Dielectric properties of $KD_2PO_4$ // J. Phys. Chem. Solids. - 1962. - Vol. 23. - P. 619-620.

[24] Volkova E.N. Physical properties of the ferroelectric $K(D_xH_{1-x})_2PO_4$ solid solutions. // Thesis submitted for the degree of candidate of sciences in physics and mathematics. Moscow, 1991, 152 p.

[25] Shuvalov L.A., Zheludev I.S., Ludupov Ts.Zh., Fiala I. // Bull. Ac. Sci. USSR, ser. phys. - 1967. - vol. 31, No 11. - p.1919-1922.

[26] Bantle W., Caflish C. Der Piezoeffekt des seignette-elektrischen Kristalls $KH_2PO_4$ // Helv. Phys. Acta. - 1943. - Vol. 16. - P. 235-250.

[27] A. Von Arx, W. Bantle, Helv. Phys. Acta, **16**, 211 (1943).

[28] A. B. Western, A.G. Baker, C.R. Bacon, V.H. Schmidt, Phys. Rev. B, **17**, 4461 (1978)

[29] V.V. Gladkii, E.V. Sidnenko, Sov. Phys. Solid State **13**, 2592 (1972).